

Evaluation Of Atomistic Simulations In Considering Alloying Effect on Strength-Toughness Trade-off Of Aluminium Alloys.

ABSTRACT:

Molecular dynamics was employed in order to evaluate its effectiveness in measuring the effect of alloying on the fracture toughness of a metal, and further gauge its accuracy in reflecting the strength-toughness trade-off of the material, with the aid of tensile deformation and crack propagation simulations. The tensile strength and the critical strain energy release rate were calculated, with a different method for the characterization of *critical* being proposed for the latter. The study is performed on Cu and Mg as alloying elements for aluminium, and vastly different effects are reported for both. The results are evaluated and further studies proposed, in order to boost the applicability of the method.

1. Introduction:

Nanomaterials have garnered significant attention in recent times due to their great applicability in the increasing miniaturization of technological components. NEMS (nano-electromechanical systems) have great potential in terms of enhancing possibilities with electrical properties, while also improving power consumption, reducing costs (as manufacturing grows in scale) and more and other aspects from the current generation of MEMS (micro-electromechanical systems). In addition, the advent of smaller mechanical components allows for greater complexity in design and, as a consequence, improved functionality [6]. Aluminium and its alloys have received interest too, due to the beneficial mechanical and electrical properties they boast [8].

A nanoscale understanding of materials is significant with regards to bulk applications as well, as it forms a foundational basis on which bulk properties can be extrapolated from the nano-level, and these compared with experimentally determined bulk properties to improve on the current understanding of these in general. Aluminium alloys, in cases of applications demanding lightweight materials, such as aerospace, are tremendously favoured due to their high strength to weight ratios. Furthermore, due to the preferred nature of the material, there has been significant progress in the manufacturing techniques involved over the last 80 odd years [9, 10].

High strength generally refers to the ability of a material to withstand significant loads without undergoing deformation of the plastic (irreversible) kind, as opposed to the elastic kind. The transition from elastic to plastic deformation is a phenomenon known as yielding, and is discussed in greater detail in Section 2. Aluminium itself does not possess greater strength than the likes of iron, but is advantageous due to its weight being less than half of most steels.

In order to increase the strength of metals, a process known as alloying is performed, which involves the mixing of metals in specific ratios to achieve a desired combination. There are numerous methods of alloying:

- Solid Solution Strengthening: this involves the placement of impurity atoms within the lattice, either as substitutes or interstitials (if the atom is significantly smaller than the matrix material).
- Grain Size Reduction: This is performed in polycrystals in order to reduce the size of individual grains (crystals).
- Precipitation Hardening: This follows the ageing of solid solution alloys, resulting in the formation of precipitates.

All of the above intend to increase the resistance to defects called dislocations, the movement of which is responsible for the yielding phenomenon. At its most fundamental level, alloying is a substitutional process - improvements in the understanding of this result in the betterment of the rest. Typical alloying elements in the case of Aluminium include Copper (2XXX series) and Magnesium (5XXX series), the effects of which are atomistically explored in this paper.

In addition to strength, an important consideration is the fracture toughness of a material. This refers to its resistance to the growth of a crack present in the material - materials on this basis are qualitatively classified as either brittle or ductile. Aluminium, like most unalloyed metals, is considered to be a ductile material (corresponding to a high toughness). However, there exists a conflict between the strength and the toughness of a material, the reason for which is that limited plastic deformation at the tip of a crack enables the dissipation of localized stress, increasing resistance to the growth of the crack. However, as strengthening is carried out, this reduces the amount of plastic deformation at a given stress level, causing a reduction in toughness [11]. No matter what the strength, the applicability of a material is reduced due to the safety hazards of a low toughness. As a consequence, careful outlining of this trade-off is important in order to optimise a material for applicability.

Simulations are powerful tools for characterizing a material before more expensive experimental tests are carried out - these involve the numerical solving of the equations constituting a model in order to obtain the result. Atomistic simulations operate on atomic level interactions, and are widely used in the field of nano-mechanics due to their ability to accurately model nanoscale materials. In addition to costs, this helps transcend several other practical constraints posed by physical testing and allows the conceptualization of properties before materials are manufactured for physical tests. Molecular dynamics is one such simulation method that formulates the physical movements of individual atoms in a material, assuming an approximated function for the potential energy between 2 (pairwise) or more (many-body) particles present. Macroscopic properties such as strength are then calculated from the summation of individual strengths, energies, or more. The software used in this study is LAMMPS (Large-scale Atomic/Molecular Massively Parallel Simulator), and results are visualized using OVITO.

The purpose of this study is to outline the characteristics of this strength-toughness trade-off in Aluminium alloys, with Cu and Mg as primary alloying elements in a set of binary-alloy single crystals. To the best of the author's knowledge, there has been no preceding atomistic study of the alloying effect on predominantly ductile metal like Aluminium, that compares this with strength. If successful, this study has the potential to be a pivotal tool in preliminary analysis of whether a high-strength alloy being designed has the toughness required to pass the safety threshold.

2. Theory:

a. Metallic Crystals

A crystalline material is characterized by a periodic array of atoms in a specific order – this is in opposition to amorphous materials that are disordered. The ordering of the atoms is known as the crystal structure, and has significant effects on the properties of the material.

The simplest structural unit is defined as the unit cell, and the repetition of this results in the formation of a large crystal. In the case of Aluminium, the unit cell is face-centred cubic (FCC) in nature. This is represented in the diagram below, and refers to atoms in the corners and faces of the cubic unit cell.

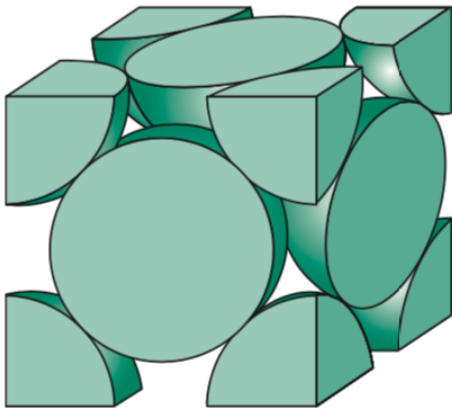


Fig. 1 [1]

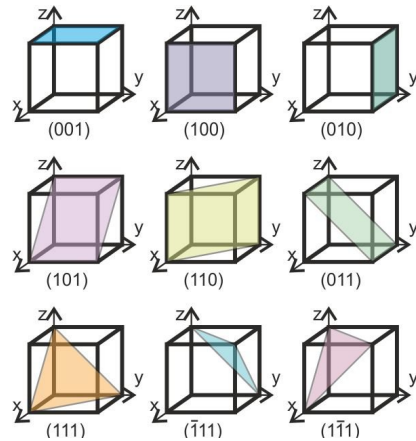


Fig. 2 [17]

Also defined is the *lattice parameter* (a_0) of a material, which refers to the edge length of the unit cell – this is same for all directions in the case of cubic unit cells.

Lastly, crystallographic planes are indicated in the notation of Miller Indices, which are essentially co-ordinates that have undergone algebraic transformations. A large portion of these, in the case of cubic cell shapes, are in Fig. 2.

b. Stress-Strain Behaviour

Engineering *strain* (ϵ) is a unitless value that quantifies the relative extension of a material, and is expressed as the change in length of a material divided by the original length.

Engineering *stress* (σ) is defined as the load (force) on a specimen divided by its original cross-sectional area, and is typically expressed as MPa or GPa (the latter will be used for this study).

When uniaxial tensile loading is applied to a material, it undergoes deformation that can be represented using a *stress-strain curve*, that appears as the following:

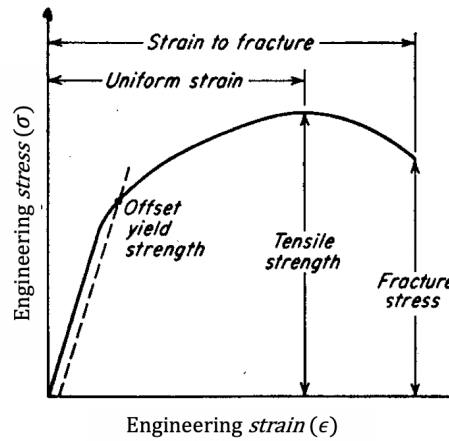


Fig. 3 [18]

The curve is initially linear, which indicates elastic deformation. This is measured by the Young's Modulus (E) of a material, which is the ratio of stress to strain in this region.

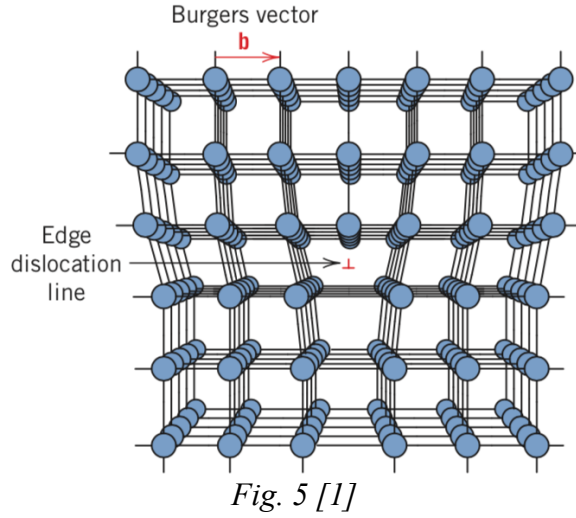
Beyond a certain point, it begins to curve (onset of plastic deformation) – the yield strength (σ_y) is a general offset measurement of this, when the linear part is reproduced at what is typically a shift to the right by strain 0.002. The ultimate tensile strength (σ_{UTS}) of a material indicates the point at which it begins to undergo breakage, either through necking, or in the case of the observations made in the MD simulations, rupture. This manifests as the maximum engineering stress on the curve.

c. Dislocations, Yielding, and Plasticity

A *dislocation* refers to a linear crystalline defect, causing a deviation from a perfect lattice structure. There exist many types of dislocations, ranging from simple “edge” or “screw” displacements to more complicated loops. Fig. 5 is a representation of an edge dislocation, in a lattice.

The burgers vector b is a means of quantifying the direction and the magnitude of the displacement found in a dislocation.

Upon the application of stress, these dislocations can move. However, this only occurs if the stress applied is equal to or greater than a critical value, beyond which it can overcome the local lattice strains. This value is known as the critically resolved shear stress (τ_c). This is a shear value because the dislocation is not necessarily parallel to the direction in which uniaxial tensile loading is applied. The movement of the dislocations is what gives rise to the phenomenon of yielding (plastic deformation), as this change is permanent and the shift in position is not restored once the load is removed.



The movement of the dislocation is known as *slip*, which can be characterized by a *slip system*. This comprises of the plane the slip takes place in, as well as the direction of it. In different lattice structures, there are different preferred systems which are most dense in their planar and linear packing. For FCC metals like Aluminium, the preferred plane is {111} and the preferred direction is <110>. The yield strength is a geometric function of τ_c , meaning it depends on the direction of the uniaxial tensile loading. Upon movement, these dislocations can build up and result in the necking/breaking of the material, that is represented by the ultimate tensile strength.

d. Fracture & Fracture Toughness

i. Introduction to Fracture

Fracture simply refers to the breaking of a material into two, as a result of the initiation and/or propagation of a crack in its crystal structure. Materials can be qualitatively characterized as ductile or brittle in order to reflect how resistant they are to fracture occurring. For ductile materials, there tends to be significant plastic deformation and absorption of energy prior to the occurrence of fracture - this is the opposite with brittle materials. As a consequence, crack propagation occurs significantly slowly in ductile materials when compared to those of the brittle kind, which is preferable in most practical applications.

ii. Modes of Fracture

The mode of fracture refers to the geometry of the crack with respect to the direction of application of stress.

Mode I fracture occurs when the stress applied is perpendicular to the direction of the crack, and this study focuses only on fracture of this type. Mode II occurs when there is in plane shear, and the crack slides. Mode III occurs when the applied shear is perpendicular to the plane, resulting in the tearing of the crack.

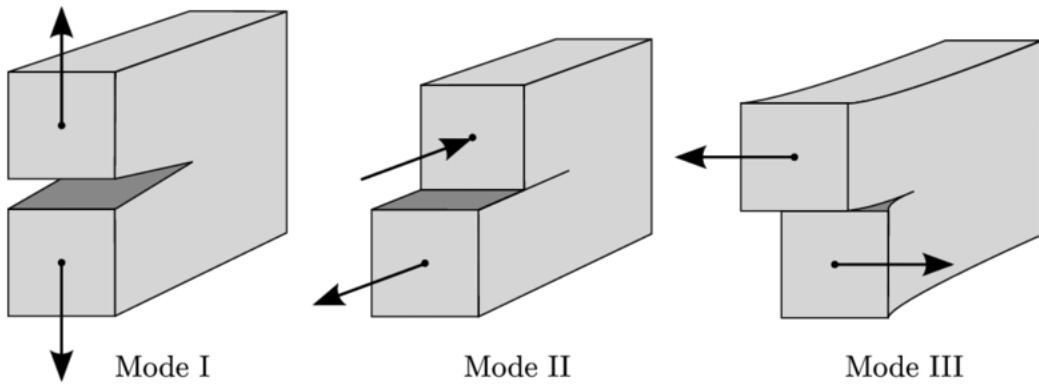


Fig. 6 [16]

iii. Introductory Fracture Mechanics

If a pre-existing crack is present in a material, it has the ability to alter the localized stresses to an extent at which it can propagate through the structure at a rapid rate, at a stress that is significantly lesser than the ultimate tensile or fracture stress. Pioneering work was carried out by A.A. Griffith, with studies involving cracks in brittle glass rods. This led to the development of the Griffith criterion for fracture.

As a crack propagates and the material splits into two, the material experiences a loss in its strain energy – the *strain energy* is defined as [20]:

$$U = \frac{\sigma^2}{2E} V$$

Here, E refers to the Young's Modulus and V to the volume of the material. The strain energy as a function of crack length, due to crack propagation is hence defined as:

$$U = \frac{\sigma^2}{2E} V - \frac{\sigma^2}{2E} (B\pi c^2)$$

Here, c refers to the length of the crack and B to the thickness of the material. Another factor is the *surface energy* of a material – since bonds must be broken to form a surface, this is a planar defect with an energy associated to it. This is defined as:

$$E_{surface} = 2\gamma_s aB$$

Here, γ_s is the surface energy per unit area. The factor of 2 arises due to cracks involving two surfaces. Hence, the total energy, as a function of crack length c , can be written as follows:

$$E = 2\gamma_s cB + \frac{\sigma^2}{2E} V - \frac{\sigma^2}{2E} (B\pi c^2)$$

This is clearly a downward-shaping quadratic function, with a critical point that would exist at a certain value of c . This can be differentiated and solved for the fracture stress in the presence of the crack, which is as follows:

$$\sigma_f = \sqrt{\frac{2\gamma_s E}{\pi c}}$$

The critical strain energy release rate (G_c) is now defined as $2\gamma_s$, as when crack propagation occurs, lost strain energy is converted to surface energy. However, this definition applies only to perfectly brittle materials, where all strain energy is converted to surface energy. When this definition was attempted for metals, significant discrepancies were found between the expected and measured values for the fracture stress σ_f . This was resolved by the addition of a second term to G_c , which accounted for energy lost to plastic deformation at the crack tip (γ_p) – the value of this term dictates the ductility of a material with positive correlation.

Hence, finally:

$$G_c = 2(\gamma_s + \gamma_p)$$

e. Solid Solution Strengthening

Alloys created in this method are generally stronger due to the misfit of impurity atoms in the primary lattice. As a consequence of the differing size of the substitutes, the presence of these atoms results in the imposition of local lattice strains, that restrict the initiation and propagation of dislocations.

These strains, and its effect on stress, can be quantified using models like the Nabarro-Lusch and Frieder-Fleischer models, that rely on misfit parameters (volume and slip), which are measures of the effect of solute elements on the stacking fault energies (the energy of a *fault* in the stacking of unit cells to form a crystal lattice) [7].

3. Methodology:

a. Molecular Dynamics

Molecular Dynamics simulations operate, as mentioned earlier, by computing the position and velocity of every particle in the simulation involved at every timestep of the simulation, using an approximated potential energy function. This is expressed using a flowchart.

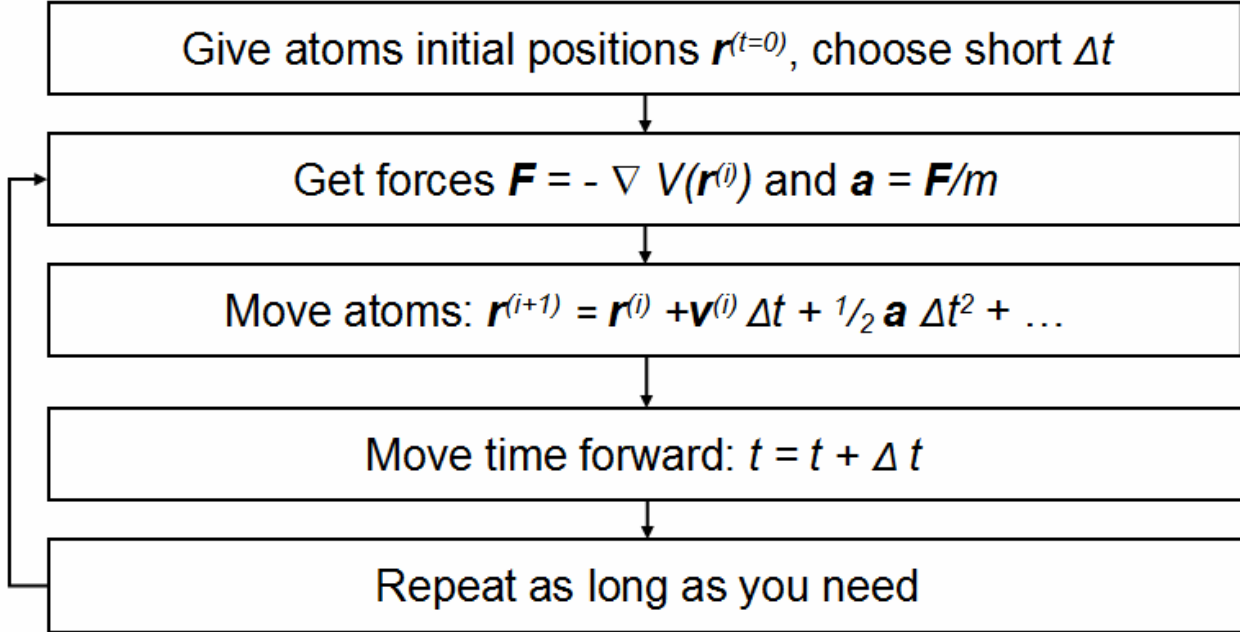


Fig. 7 [19]

Aspects that are crucial to the accuracy of the simulation are the selection of (i) an appropriate potential function, and (ii) an appropriate numerical integration algorithm - these have a significant impact on the trajectories found, and as a consequence the results as a whole. This study uses the LAMMPS software [2], which relies on the velocity Verlet algorithm in the simulations performed. This algorithm uses one force computation every timestep and hence has significant accuracy in position and velocity.

This study uses Embedded-Atom-Method (EAM) interatomic potentials in order to compute the force between any two particles in the system involved. This selection is due to the greater suitability of the many-body EAM, and the reliability outlined by most studies in literature operating with metallic crystals. In this, the energy is expressed as a sum of functions of the distance between an atom and all its neighbours.

For the Al-Cu binary system, the potential developed by Liu, Liu, and Borucki was used [4]. For the Al-Mg binary system, the potential developed by Liu and Adams was used [5]. All visualizations were carried out using the OVITO software [3].

b. Basic Analytical Concepts - Toughness

Toughness, for this investigation, was considered to be measured by G_c . The calculation of G_c was carried out in a manner identical to that used by Zhuo (et al) [13]. This method subscribes to the definition of the strain energy release rate as the available energy for the incrementation of a crack, per unit thickness, and hence is expressed as:

$$G = \frac{\Delta U(c)}{B \Delta c}$$

Here, $U(c)$ is the strain energy at a particular crack length, and B is the thickness of the material (which remains constant). $U(c)$ is defined as follows:

$$U(c) = E(c) - E_0(c)$$

Here, $E(c)$ is the potential energy at a particular load, and $E_0(c)$ is the potential energy when no load is present. Since the smallest incrementation of crack length occurs with an increase of $0.5a_0$, Δc is $0.5a_0$ (2.023\AA). The values for $E(c)$ are calculated at each strain level, and $E_0(c)$ is independently determined after equilibration for each crack length ($20a_0$ and $20.5a_0$).

The reason for not considering calculated values for γ_p directly, and considering the critical value for G instead, is that it was observed that the surface energy γ_s also changed as alloying was performed, due to the different energy of the now more common Al-Cu or Al-Mg bonds. Hence, this would not have been a reflective value of the overall toughness of the material.

c. Computational Details

The lattice parameter (a_0) for pure Aluminium was set as 4.046\AA , and a simulation box was created with the dimensions $48a_0 \times 48a_0 \times 5a_0$, where the geometry of crystal orientations is [100], [010], and [001] in the x, y, and z dimensions, respectively. In order to generate uniform distributions of alloying elements, the substitution was performed in a 2-step process. First, a smaller box with dimensions $4a_0 \times 4a_0 \times 5a_0$ was made, containing 320 atoms. The random substitutions were then carried out at alloying percentages 2.5%, 5%, 7.5%, 10%, and 15%. Following this, the resultant lattice was multiplied by a factor of 12 in the x and y dimensions, resulting in a total of 46020 atoms. In order to ensure consistency with both Cu and Mg as alloying elements, the positions of the atoms where these substitutions were carried out were identical.

While nanorods or nanowires are typically implemented in tensile deformation simulations [12], a slab like structure was adopted in both crack propagation and tensile deformation simulations to ensure consistency amongst both.

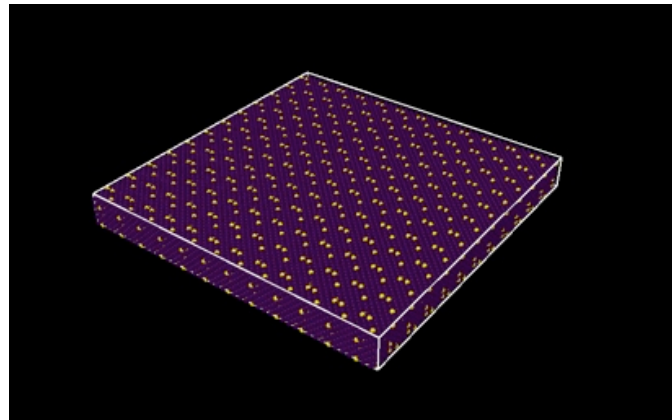


Fig. 8: Al with Cu at 5% (yellow atoms = Cu, purple atoms = Al)

In both tensile deformation and crack propagation simulations, strain was applied along the x-direction using a method involving the assignment of a layer $3a_0$ wide on either end as a boundary

wall. The forces were set to zero in the wall spaces, and deformation was performed by the movement of the boundary wall at a fixed speed. This is similar to experimental techniques of uniaxial tensile loading, and is expected to yield better results.

However, considering the timescale of MD simulations in general, the strain rate involved is very high, as opposed to what is practical. A timestep of 0.002ps was selected in both simulations, and this was run for a totality of 40ps, with the goal of approximately achieving strain 0.2. Given the computational times, the wall was set to move at 1\AA ps^{-1} , which is equal to 100 m/s. The effect of high strain rate on results obtained is a well-documented phenomenon, and the rate involved here gives rise to mixed-mode deformation, that involves both deformation in a crystalline fashion (dislocations etc.) as well as deformation that results in the atoms being disordered, or amorphous. Typically, this is indicative of relatively low accuracy in terms of results – however, given the lack of access to a parallel computer network, with just a single-processor laptop involved in the computations, this was reasonable. Nonetheless, this is a significant limitation observed.

- *Tensile Deformation Simulations:*

Periodic boundary conditions were applied in the y and z directions – this was so that pressure equilibration could be carried out in the y-direction, which appeared to begin with significant initial pressure otherwise. Periodic conditions refer to a state when one particle leaves the simulation box.

The simulation took place in two stages. First, there was an equilibration process carried out for a duration of 10ps, under NPT (isothermal-isobaric) conditions. The number of molecules (N), the pressure in specified perpendicular directions (P), and the temperature (T) was fixed – this was performed at a temperature of 300K, and the pressure in the y and z direction was set to zero. Next, deformation was carried out under NVT (canonical) conditions, where volume is preserved instead of pressure, for a duration of 40ps. This selection was made in order to preserve box geometry as deformation was carried out, as well as the fact that simulations using NPT for this stage resulted in abnormal behaviour of the atoms near the region of the moving wall, which occurred due to the program's attempt to keep pressure in y set to 0.

The results for the simulation were also obtained at a significantly lower timestep of 0.0005ps, and these agreed with the 0.002ps simulations to 3 decimal places in the case of σ_{UTS} . Hence, the lower computational intensity was deemed acceptable.

The temperature equilibration is performed using a Nose-Hoover thermostat, which performs this by the coupling of dynamic variables to the velocity variables.

- *Crack Propagation Simulations:*

Here, it was opted to simulate an edge crack. The crack was oriented in the [010] direction, and deformation applied across the [100] direction. Its creation involved the selection of all the atoms to the left and right of the simulation box centreline, up to the pre-set crack length, and the subsequent elimination of all interactions between these. As a consequence, the crack did not

rebind when equilibration was performed, which was not the case when the removal of atoms was attempted instead.

Zhang opted to use the NVE (microcanonical) ensemble [15], which conserves energy rather than temperature, in order to measure energy changes accurately, without losing energy to the thermostat applied. However, significant fluctuations in temperature were observed, which have an effect on the crack tip processes being studied (----). Hence, NVT conditions were applied in both the equilibration (10ps) and deformation (40ps) phases, with a temperature of 10K to minimize temperature effects on the ductility of the material.

4. Results & Discussion:

a. Tensile Deformation

i. Analytical Walkthrough

The stress was calculated by LAMMPS by computing the sum of all per-atom stresses in the x-direction. In order to do this, stress was defined as *virial*. This is an atomic level measure of mechanical stress that excludes the kinetic energy, and is expressed as follows:

$$\tau_{ij} = \frac{1}{\Omega} \sum_{k \in \Omega} \left(-m^{(k)} (u_i^{(k)} - \bar{u}_i)(u_j^{(k)} - \bar{u}_j) + \frac{1}{2} \sum_{\ell \in \Omega} (x_i^{(\ell)} - x_i^{(k)}) f_j^{(k\ell)} \right)$$

Strain was computed using the definition cited in Section 2. Next, a stress-strain curve was plotted using Microsoft Excel. Fig. 9 displays the curve found for pure Aluminium, when the Al-Cu EAM potential was employed.

Due to a shift in temperature after equilibration, the cause of which could not be ascertained, there was initial non-linearity and compressive (negative) stress. Hence, it was decided to disregard the offset yield strength of the material and focus only on the ultimate tensile strength instead. This was ascertained by selecting a region of data points near the point of maximum stress, and approximating the curve using a 4th-order polynomial function – Fig. 9 shows the results for pure Al using the Al-Cu EAM potential, that has a R² value of 0.9911. The R² value is a measure of how closely the data points are approximated by the fit assigned, and values greater than 0.99 are generally significant results. The local maximum was then found, and this was assigned to be the ultimate tensile strength of the material. Here, the value was 5.850 GPa.

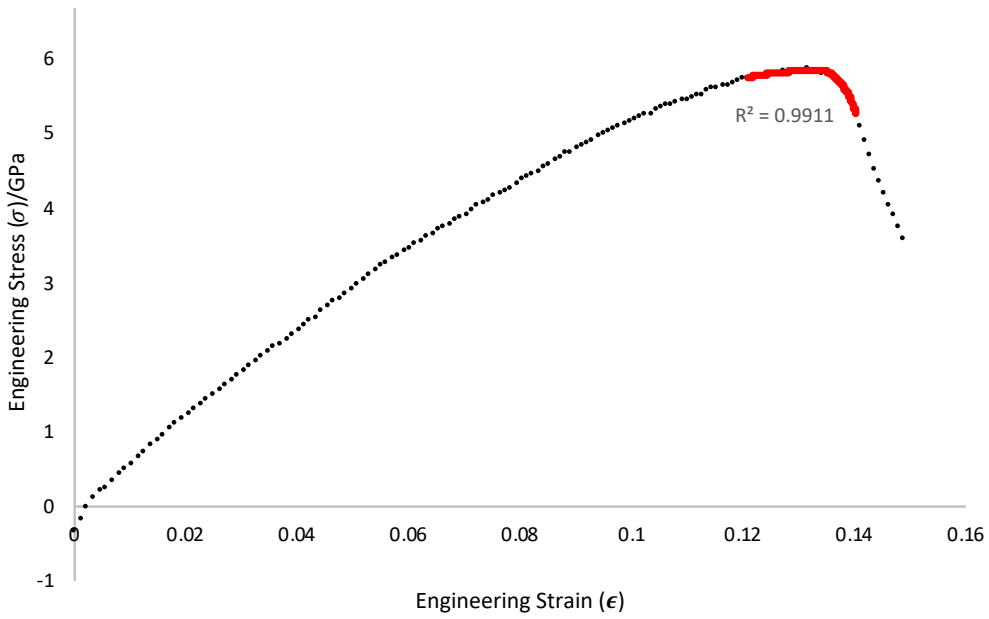


Fig. 9

ii. Data

COPPER			
<i>At.%</i>	σ_{UTS}/Gpa	$\Delta\sigma_{UTS}/Gpa$	% $\Delta\sigma_{UTS}$
0.0	5.850	0	0.000
2.5	5.883	0.033	0.564
5.0	6.039	0.189	3.231
7.5	6.063	0.213	3.641
10.0	6.210	0.360	6.154
15.0	6.303	0.453	7.744

Table 1a

MAGNESIUM			
<i>At.%</i>	σ_{UTS}/Gpa	$\Delta\sigma_{UTS}/Gpa$	% $\Delta\sigma_{UTS}$
0.0	7.813	0	0.000
2.5	7.559	-0.254	-3.254
5.0	6.817	-0.996	-12.748
7.5	6.986	-0.828	-10.592
10.0	6.792	-1.021	-13.072
15.0	6.523	-1.290	-16.510

Table 1b

In the case of the Magnesium values, there was significant initial compressive stress in the system that increased with the alloy percentage. In order to achieve consistency with the Copper system that did not experience this, the values for the stress were increased by the initial offset. In addition, due to the significant difference in the values for pure Aluminium when different potentials were used, the change in stress as a consequence of the alloying is evaluated, and further a percentage change is evaluated.

Contrary to expectation, the tensile strength of Mg-alloyed Al tended to clearly *decrease* with an increase in alloying percentage. It is suspected that this result is a combination of the computational design used coupled with the potential used; however, seeing as the effects were consistent with prediction in the case of Cu as the alloying element, it is difficult to ascertain the cause, especially considering both use well established EAM potential. Further study is required here.

b. Crack Propagation

i. Analytical Walkthrough

The analytical procedure followed here was identical to that outlined in Section 3. One identified key aspect for consistency is the decision of what the critical point in the strain energy release rate is. In the case of Zhuo (et. al), the point preceding a sharp drop in the tensile stress was used, despite the fact that this may have occurred a few timesteps *after* the propagation had already occurred. When this method was tested in this study, inconsistent results were observed as the alloying percentage was changed – the stress-strain curve found developed two local maxima, and the point of propagation did not coincide with either.

Instead, the visualizations of the simulation were carefully analysed and the timestep characterizing full propagation of the crack by a distance of $0.5a_0$ was kept as the critical point – this resulted in consistent values and conformed with the predictions outlined.

The process of ascertaining the critical point, for pure Aluminium with the use of the Al-Cu potential, are displayed below.

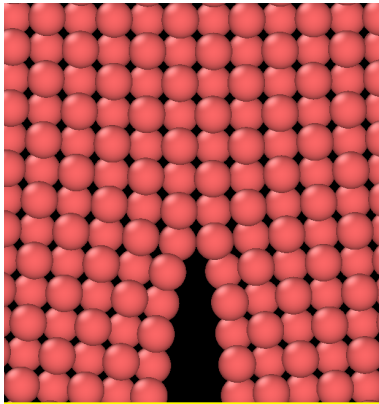
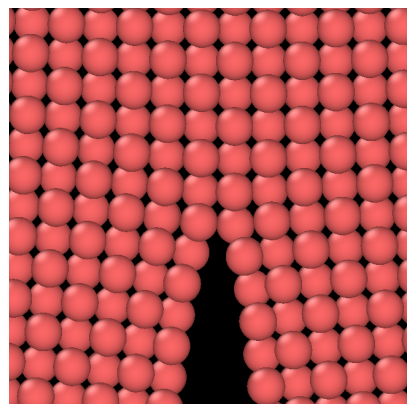


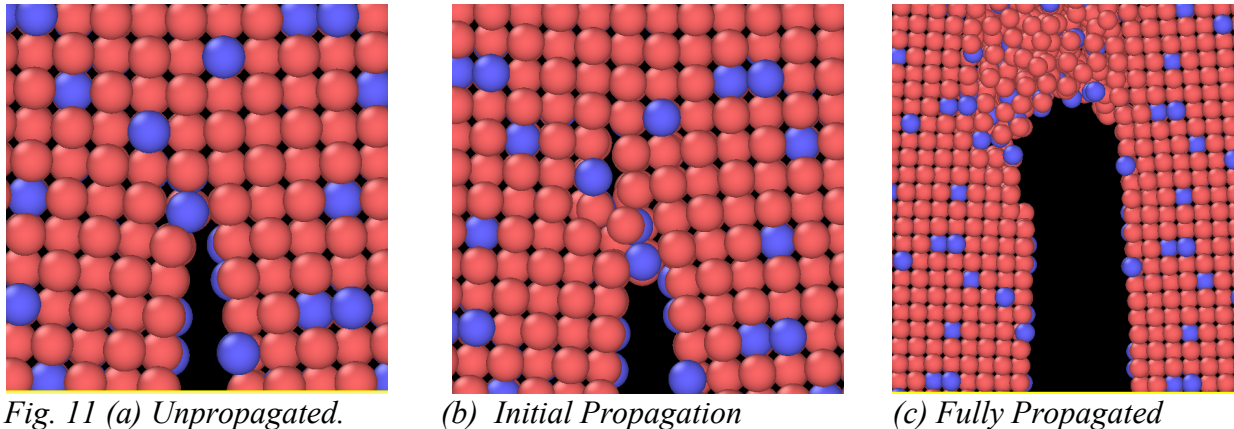
Fig. 10: (a) Unpropagated Crack



(b) Crack Propagated by $0.5a_0$

The selected timestep was the one that immediately preceded the state in X(b), and reflected the state just before the crack has truly increased in surface area corresponding to the smallest possible length increase.

However, in several cases where an alloying element was added, the propagation of the crack was not as straightforward. Pictured below is the observation made for 10% Al-Mg.



In this case, the critical point was declared to be the point at which propagation carries forth with a non-tip atom, when the force between the first set of pairs is fully terminated.

LAMMPS outputs energy in eV. Upon the calculation of the strain energy release rate, this value was in $\text{eV}\text{\AA}^{-2}$. This was multiplied by a factor of 16.0218 in order to correct the units to Jm^{-2} .

ii. Data

COPPER			
<i>At. %</i>	G_c/Jm^{-2}	$-\Delta G_c/\text{Jm}^{-2}$	$\%\Delta G_c$
0.0	1.478	0	0.000
2.5	1.352	-0.126	-8.525
5.0	1.199	-0.279	-18.877
7.5	1.147	-0.331	-22.395
10.0	0.953	-0.525	-35.521
15.0	-1.819	-3.297	-223.072

Table 2a

MAGNESIUM			
<i>At. %</i>	G_c/Jm^{-2}	$\Delta G_c/\text{Jm}^{-2}$	$\%\Delta G_c$
0.0	1.716	0	0.000
2.5	1.590	-0.126	-7.343
5.0	1.339	-0.377	-21.970

7.5	1.268	-0.448	-26.107
10.0	1.115	-0.601	-35.023
15.0	0.570	-1.146	-66.783

Table 2b

It should be noted that for the Cu-alloyed aluminium with 15% atom percentage, equilibration resulted in significant initial stress and a curved crack, causing propagation from the first timestep. This value was deemed unreliable and ignored in further analysis. This is suspected to be a consequence of the significantly increased presence of Cu atoms, distorting the potential energies of atoms surrounding the crack, and hence the calculated stress. This should not be a consideration in real materials. Moreover, degree of drop-off is greater for Mg than for Cu, although the contrary would be expected considering the difference in atomic size. However, due to the unreliable measurements for Mg strength, this can be qualified as erroneous.

c. Strength vs. Toughness

i. Trade-Off Data

The trade-off is tabulated below for both sets (Cu & Mg). Here, the change in percentage is shown instead, due to the differing initial values.

COPPER		
At.%	% $\Delta\sigma_{UTS}$	% ΔG_c
0.0	0.000	0.000
2.5	0.564	-8.525
5.0	3.231	-18.877
7.5	3.641	-22.395
10.0	6.154	-35.521
15.0	7.744	-223.072

Table 3a

MAGNESIUM		
At.%	% $\Delta\sigma_{UTS}$	% ΔG_c
0.0	0.000	0.000
2.5	-3.254	-7.343
5.0	-12.748	-21.970
7.5	-10.592	-26.107
10.0	-13.072	-35.023
15.0	-16.510	-66.783

Table 3b

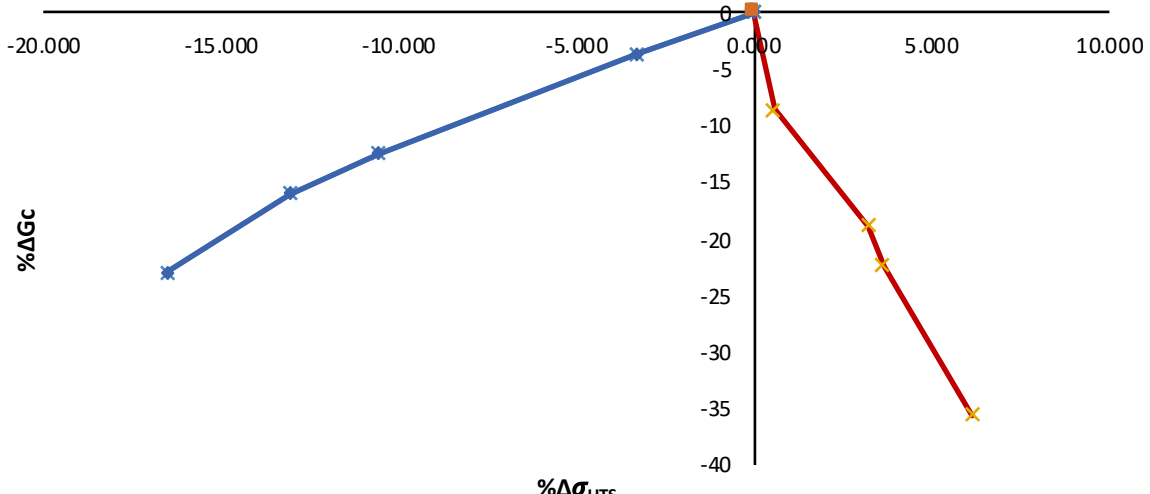


Fig. 12

The red line indicates the variation for Al-Cu, while the blue-line indicates that for Al-Mg. In both cases, there appears to be a relatively linear progression of $\% \Delta G_c$ with $\% \Delta \sigma_{UTS}$, albeit in different directions. When a linear fit is applied to the trend for Al-Cu, the obtained R^2 value is 0.9779, which is acceptable given the preliminary nature of this study. The gradient found considering these relatively large differences in concentration is $-5.373 \text{ Jm}^{-2}/\text{GPa}$, which clearly is significant in terms of the trade-off found. This can be further investigated with rigorous testing at smaller concentration differences.

ii. Discussion

Due to the significant difficulty involved in quantifying error and uncertainty from molecular dynamics simulations, which still is an ongoing field of research, the evaluations made are only qualitative.

It is expected that a major cause from deviation from prediction, especially in the case of Magnesium alloying which has been documented as successful in polycrystals with the aid of Molecular Dynamics, was the high strain rate involved. This generally resulted in a high degree of amorphous (disordered) yielding, with negligible necking observed. However, given the limited computational power available, this was not easily adjustable.

This also potentially compromised results pertaining to the plasticity observed at the crack tip, where disorder was also observed to be predominant. The Dislocation Analysis Tool (DXA) on OVITO certainly recorded dislocations in both of these cases, but the transition to disorder was far more predominant, as seen in the figure below.

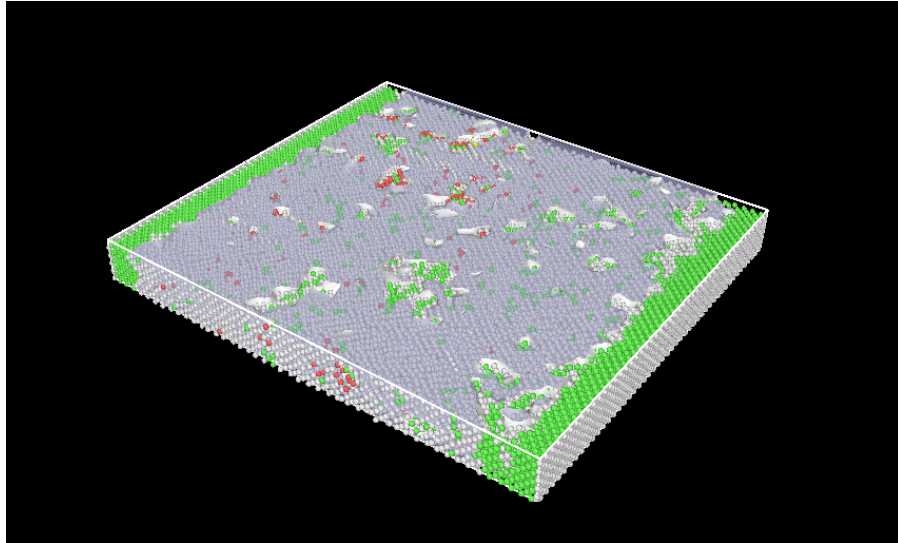


Fig. 13

The white region indicates an atom with no particular crystal arrangement, and here forms 77.3% of all atoms. In this same frame, 19 dislocations were identified by the software, but considering the significant disorder in the system, these clearly are not the dominating mechanism.

Nonetheless, results have been obtained with a trend similar to expectation, clearly indicating the potential for MD to be a useful tool in considerations of toughness when developing new single or polycrystal materials.

The Copper trade-off level is quite high, and it is unclear as to whether this entirely is a function of strain rate or any other deciding factors. As a result, careful studies involving first the impact of MD simulation parameters, and then the correlation of these results to physical experiments, under a vast set of conditions must be carried out. Upon sufficient testing, a quantitative framework for extrapolating MD results and comparing them with reality can be established – both for toughness and strength. It is worth noting that in preliminary stages where this quantitative framework is unestablished, it is worth carrying out simulations to obtain qualitative understandings of potential new materials too. Lastly, along with the above, the author believes it is significant to also conduct studies focusing on crack tip plasticity and drawing correlations to calculated quantities such as toughness.

5. Conclusion

Although the results partly present significant deviation from expected results, they clearly demonstrate that alloying studies of crack propagation and fracture mechanics can be performed using Molecular Dynamics. The strength trend for Copper as the alloying element was linear, consistent with the results found for polycrystals [14]. In order to further develop the method and make it reliable, careful consideration must be given to the standardisation of a temperature at which these are carried out, as well as ensembles, deformation mechanisms, crack generation methods, and substitution methods. Furthermore, a study of the effect of strain rate on the toughness values, with and without considering the effect on strength should be performed in order to optimise this method.

6. References

1. Callister, William D., and David G. Rethwisch. *Materials science and engineering: an introduction*. Vol. 7. New York: John Wiley & Sons, 2007.
2. Plimpton, Steve. "Fast parallel algorithms for short-range molecular dynamics." *Journal of computational physics* 117.1 (1995): 1-19. (<https://lammps.sandia.gov/index.html>)
3. Stukowski, Alexander. "Visualization and analysis of atomistic simulation data with OVITO—the Open Visualization Tool." *Modelling and Simulation in Materials Science and Engineering* 18.1 (2009): 015012.
4. Liu, X-Y., C-L. Liu, and L. J. Borucki. "A new investigation of copper's role in enhancing Al–Cu interconnect electromigration resistance from an atomistic view." *Acta materialia* 47.11 (1999): 3227-3231.
5. Liu, X-Y., and J. B. Adams. "Grain-boundary segregation in Al–10% Mg alloys at hot working temperatures." *Acta Materialia* 46.10 (1998): 3467-3476.
6. <https://people.eecs.berkeley.edu/~ctnguyen/Research/PlenaryTalks/SmallerIsBetter.mit-marc06.ctnguyen.pdf>
7. Ma, Duancheng, et al. "Ab initio study of compositional trends in solid solution strengthening in metals with low Peierls stresses." *Acta Materialia* 98 (2015): 367-376.
8. Fujii, Takashi, et al. "Controlled morphology of aluminium alloy nanopillar films: from nanohorns to nanoplates." *Nanotechnology* 21.39 (2010): 395302.
9. Dursun, Tolga, and Costas Soutis. "Recent developments in advanced aircraft aluminium alloys." *Materials & Design (1980-2015)* 56 (2014): 862-871.
10. Mouritz, Adrian P. *Introduction to aerospace materials*. Elsevier, 2012.
11. Ritchie, Robert O. "The conflicts between strength and toughness." *Nature materials* 10.11 (2011): 817.
12. Liu, Yongli, et al. "Molecular Dynamics Study of the Tensile Deformation on Aluminium nanorod." *2016 4th International Conference on Sensors, Mechatronics and Automation (ICSMA 2016)*. Atlantis Press, 2016.
13. Zhuo, Xiao, Jang Kim, and Hyeon Beom. "R-curve Evaluation of Copper and Nickel Single Crystals Using Atomistic Simulations." *Crystals* 8.12 (2018): 441.
14. Hocker, Stephen, et al. "Molecular dynamics simulations of tensile tests of Ni-, Cu-, Mg- and Ti-alloyed aluminium nanopolycrystals." *Computational Materials Science* 116 (2016): 32-43.
15. Zhang, Jiaxi. *Molecular dynamics study of crack propagation behavior and mechanisms in nickel*. Diss. The Ohio State University, 2011.
16. Kammer, D. *Slip fronts at frictional interfaces: A Numerical and Theoretical Study*. Diss. PhD Thesis (EPFL Lausanne, 2014).
17. Waeselmann, Naëmi. "Structural transformations in complex perovskite-type relaxor and relaxor-based ferroelectrics at high pressures and temperatures." (2012).
18. <http://www.ctia.com.cn/Technology/2009/24643.html>
19. Safont Camprubí, Gemma. "Mechanical properties at nano-level." (2010).
20. <https://www.fracturemechanics.org/griffith.html>